

Effective Potentials, Energies, and Pair-distribution Functions of Plasmas by Monte-Carlo Simulations

H. WAGENKNECHT, W. EBELING, A. FÖRSTER

Institut für Physik, Humboldt-Universität zu Berlin,
Invalidenstraße 110, D-10115 Berlin, Germany
e-mail: ebeling@physik.hu-berlin.de

Received 17 April 2000, in final form 2 October 2000

Abstract

The one-component plasma (OCP), an electron gas on a positive background, and the subsystem of free charges in a two-component plasma (TCP) is investigated using a quasi-classical approach. Quantum effects such as the Heisenberg uncertainty principle and the Pauli exclusion principle are incorporated into our model by effective potentials. In case of the OCP the symmetry effects are of special interest whereas in case of TCP the Heisenberg effects play the significant role. The method of Slater sums is used to obtain effective potentials. Monte Carlo simulations for both OCP and TCP were carried out to calculate the Coulombic energy, the effective energy, and the pair-distribution functions.

1 Introduction: systems of charged fermions

The description of many-particle systems of charged fermions belongs to the most interesting problems in modern physics. Such a description can be made either in the physical or in the chemical picture. In the physical picture the system consists of electrons and nuclei only and it is completely determined by the Coulomb interaction of these point-like particles and their statistics.

In the chemical picture the description of the system is more complex. It is composed of free electrons, free nuclei, and different types of bound states such as ions, atoms, and molecules. All these particles are introduced as individual "chemical species" which interact by effective pair potentials. Although the treatment of a plasma within the chemical picture yields a good description of the system it is essential to carry out a careful quantum-mechanical calculation of all different types of effective pair potentials. This way a double counting of effects can be avoided.

We investigate a plasma in the region of partial degeneration and strong coupling. The next section gives an introduction of effective pair potentials. In section 3 we present results for the simulations of an electron gas which is of interest in solid state physics and which has been investigated by many researchers, e.g. [1]-[4]. In section 4 results for the mass-symmetrical plasma are given. Such systems may be observed in semiconductors [5] or in astrophysics [6]. At the temperatures of the simulations the plasma is almost fully ionised and hence interactions between bound states and free charges are thermodynamically insignificant. For our investigation we restrict ourselves to a system of free electrons (index e) and free positrons (index p).

2 Effective potentials

2.1 Coordinate-dependent potentials

Effective potentials can be obtained by the method of Slater sums which was already used by Morita [7] and was further developed by Kelbg [8], Ebeling *et al.* [9] and Rohde *et al.* [10]. All quantum effects are included into an effective pair potential by modification of the original Coulomb energy U^{Coul} to an effective energy:

$$\frac{e_i e_j}{4\pi\epsilon_0 r_{ij}} \rightarrow \frac{e_i e_j}{4\pi\epsilon_0 r_{ij}} F(r_{ij}, m_{ij}, T), \quad (1)$$

$$\text{where } r_{ij} = |\vec{r}_i - \vec{r}_j| \quad \text{and} \quad m_{ij} = \frac{m_i m_j}{m_i + m_j}.$$

The effective potential of the particle i with respect to the position of the particle j is obtained by dividing the effective energy by the charge e_j . The effective potential depends not only on the distance between particles like the Coulomb potential but it depends also on the temperature T and on the masses of particles m_i, m_j . At high temperatures perturbation theory yields in first order [8]

$$F(r_{ij}, m_{ij}, T) = 1 - \exp\left\{-\frac{r_{ij}^2}{\lambda_{ij}^2}\right\} + \sqrt{\pi} \left(\frac{r_{ij}}{\lambda_{ij}}\right) \left[1 - \text{erf}\left(\frac{r_{ij}}{\lambda_{ij}}\right)\right], \quad (2)$$

where λ_{ij} denotes the thermal de Broglie wavelength given by $\lambda_{ij} = \hbar/\sqrt{2m_{ij}k_B T}$, \hbar is the Planck constant and k_B is the Boltzmann constant. This way we find the Kelbg interaction energy U_{ij}^{K}

$$U_{ij}^{\text{K}} = \frac{e_i e_j}{4\pi\epsilon_0 r_{ij}} F(r_{ij}, m_{ij}, T). \quad (3)$$

We assume that for the two-component plasma (TCP) of free charges the quasi-classical Hamiltonian has the form

$$H = \sum_{i=1}^N \frac{p_i^2}{2m_i} + \sum_{i<j} U_{ij}^{\text{K}}. \quad (4)$$

Here $i, j = 1 \dots N$ are the indices of the particles and N is the total number of particles. We restrict our investigation to temperatures $T \geq 10^4 K$, consider only the free charges, and we assume that the real interactions have the same functional form as the Kelbg potential with an additional free parameter γ_{ij} . The function $F(r_{ij}, m_{ij}, T)$ in Eqs.(3) is replaced by $F(r_{ij}, m_{ij}, T, \gamma_{ij})$ which is defined as

$$F(r_{ij}, m_{ij}, T, \gamma_{ij}) = 1 - \exp\left\{-\frac{r_{ij}^2}{\lambda_{ij}^2}\right\} + \sqrt{\pi} \left(\frac{r_{ij}}{\lambda_{ij} \gamma_{ij}}\right) \left[1 - \text{erf}\left(\gamma_{ij} \frac{r_{ij}}{\lambda_{ij}}\right)\right]. \quad (5)$$

For $\gamma_{ij} = 1$ Eq.(5) coincides with Eq. (2). Now we use the method of Slater sums to correct the height of the Kelbg potential at zero-point distance [9]

$$\frac{e_i e_j}{4\pi\epsilon_0 r_{ij}} F(r_{ij} = 0, m_{ij}, T, \gamma_{ij}) = -k_B T \ln [S_{ij}(r_{ij} = 0)] \quad (6)$$

and simultaneously to conserve the correct first derivative for $r \rightarrow 0$

$$\frac{e_i e_j}{4\pi\epsilon_0} \left[\frac{1}{\lambda_{ij}^2} - \frac{2}{\lambda_{ij} \gamma_{ij}} \frac{\gamma_{ij}}{\lambda_{ij}} \right] = -\frac{e_i e_j}{4\pi\epsilon_0} \frac{1}{\lambda_{ij}^2}. \quad (7)$$

In Eq. (6) S_{ij} denotes the binary Slater sum of the particles i and j at zero distance including also symmetry effects coming from the different spin directions. It is given by

$$S_{ep}(r_{ep} = 0) = \sqrt{\pi} \xi_{ep}^3 [\zeta(3) + \xi_{ep}^2 \zeta(5)] + 4\sqrt{\pi} \xi_{ep} \int_0^\infty e^{-x^2} \frac{x dx}{1 - \exp\left\{-\frac{\pi \xi_{ep}}{x}\right\}}, \quad (8)$$

$$S_{ee}(r_{ee} = 0) = S_{pp}(r_{pp} = 0) = 2\sqrt{\pi} \xi_{ee} \int_0^\infty e^{-x^2} \frac{x dx}{1 - \exp\left\{-\frac{\pi \xi_{ee}}{x}\right\}}. \quad (9)$$

Values for the logarithm of the binary Slater sums for different temperatures are given in Tab. 1. The interaction parameter ξ_{ij} is defined by $\xi_{ij} = -e_i e_j / (4\pi\epsilon_0 \lambda_{ij} k_B T)$. In Eq.(8) for the bound states the Brillouin-Planck-Larkin convention is used. $\zeta(k)$ denotes Riemann's Zeta-function. In Eq.(9) the symmetry effects coming from different spin directions of electrons and positrons are already included.

From Eq. (6) the parameter γ_{ij} can be calculated for $r_{ij} = 0$. It is given by

$$\gamma_{ij} = -\frac{\sqrt{\pi}}{\lambda_{ij}} \frac{e_i e_j}{4\pi\epsilon_0 k_B T \ln [S_{ij}(r_{ij} = 0)]}. \quad (10)$$

Eq. (7) is identically fulfilled which means that the first derivative of the effective potential energy Eqs. (4,5) is correct for $r_{ij} = 0$. This identity is fulfilled only for the given argument in the error-function in Eq.(5).

The advantage of effective potentials derived from Slater sums is that the pair-correlations and the thermodynamic functions can be described correctly. On the other hand the momentum distributions in computer simulations with these effective potentials are always Maxwell distributions. This may be corrected by another type of potential - the momentum-dependent potential which will be introduced in the next subsection.

T/K	$\ln(S_{ee}(r=0))$	$\ln(S_{ep}(r=0))$
10000	-9.04071	7.99727
20000	-6.84912	6.4018
30000	-5.82477	5.51923
40000	-5.19576	4.92503
50000	-4.75786	4.48641
60000	-4.42984	4.14441
70000	-4.17197	3.86776
80000	-3.96216	3.63795
90000	-3.78702	3.44311
100000	-3.63788	3.27526

Tab. 1: Logarithm of the binary Slater sums for different temperatures

2.2 Momentum-dependent potentials

Momentum-dependent effective potentials may be obtained from the Gaussian wave-packets (GWP) approach. In this case the quasi-classical Hamiltonian has the following structure

$$H = \sum_{i=1}^N \frac{p_i^2}{2m_i} + \sum_{i<j} U^P \left(\frac{r_{ij}}{r_0}, \frac{p_{ij}}{p_0} \right) + \sum_{i<j} \frac{e_i e_j}{4\pi\epsilon_0} F \left(\frac{r_{ij}}{r_0} \right), \quad (11)$$

with $p_{ij} = |\vec{p}_i - \vec{p}_j|$. The interaction between two particles in a surrounding plasma is modelled in two ways, first by the Pauli energy U_P and second by an effective Coulomb energy that is determined by a certain function $F(r_{ij}/r_0)$. Starting with a GWP

$$\Psi_0(\vec{x}) = \left(\frac{1}{\pi\sigma^2} \right)^{3/4} \exp \left\{ -\frac{(\vec{x} - \vec{r})^2}{2\sigma^2} + \frac{i\vec{p} \cdot (\vec{x} - \vec{r})}{\hbar} \right\} \quad (12)$$

effective expressions of type Eq.(11) are obtained by averaging the Hamilton operator with respect to $\Psi_0(\vec{x})$,

$$H = \int d\vec{x} \Psi_0^*(\vec{x}) \hat{H} \Psi_0(\vec{x}). \quad (13)$$

An effective momentum-dependent Pauli energy can be obtained when averaging the operator of the kinetic energy with respect to an antisymmetrised two-particle wave function of identical particles. The Pauli energy has the form

$$U^P = U_0 \exp \left(-\frac{\Delta_{ij}^2}{2} \right) \quad \text{with} \quad \Delta_{ij}^2 = \left(\frac{r_{ij}}{r_0} \right)^2 + \left(\frac{p_{ij}}{p_0} \right)^2 \quad (14)$$

and was already suggested by Dorso *et al.* [11] and was used by Klakow *et al.* [12] and Ebeling *et al.* [13]. Here p_0, r_0 , and U_0 are parameters which satisfy the conditions $p_0 r_0 = \hbar$ and $U_0 = \hbar^2 / (4m_e r_0^2) = c k_B T$. m_e is the electron mass. The constant c can be obtained from the calculation of the pair-correlation function of the ideal gas

$$g(r) = \frac{1}{(2\pi m k_B T)^3} \int d\vec{p}_1 d\vec{p}_2 \exp \left\{ -\frac{H}{k_B T} \right\} \quad (15)$$

and fitting $g(r = 0)$ at zero distance to the exact value $g(r = 0) = 1/2$ for the ideal Fermi gas

$$g_{r=0} = \frac{1}{2} = \frac{1}{2\sqrt{\pi}} \left(\frac{8U_0}{k_B T} \right)^{3/2} \int_0^{\infty} dp p^2 \exp \left\{ -p^2 \left(\frac{2U_0}{k_B T} \right) \left(\frac{\exp(p^2) - 0.5}{\exp(p^2) - 1} \right) \right\}. \quad (16)$$

This condition yields the value $c = 1.015819$. Furthermore, by the averaging procedure Eq.(13) an effective Coulomb energy of the form

$$U_{ij}^{\text{KTR}} = \frac{e_i e_j}{4\pi\epsilon_0} F \left(\frac{r_{ij}}{r_0} \right) = \frac{e_i e_j}{4\pi\epsilon_0 r_{ij}} \operatorname{erf} \left(\frac{r_{ij}}{\sqrt{2\pi} \lambda_{ij}} \right) \quad (17)$$

is obtained which was already used by Klakow, Toepffer, and Reinhard [12] and Ebeling *et al.* [13]. The KTR potential does not provide a correct description of the spatial correlations at small distances. This deficit may be corrected by a combination of the KTR potential with the method of Slater sums. To receive the correct potential energy at zero-point distance we propose a modification of the argument of the error function in Eq.(17). The modified effective Coulomb energy reads

$$U_{ij}^{\text{KTR,corr}} = \frac{e_i e_j}{4\pi\epsilon_0} F \left(\frac{r_{ij}}{r_0} \right) = \frac{e_i e_j}{4\pi\epsilon_0 r_{ij}} \operatorname{erf} \left(\frac{r_{ij}}{R_{ij}^*} \right). \quad (18)$$

In this expression R_{ij}^* is given by

$$R_{ij}^* = -\frac{2}{\sqrt{\pi}} \frac{e_i e_j}{4\pi\epsilon_0} \frac{1}{k_B T \ln [S_{ij}^0(r_{ij} = 0)] + U^{\text{P}}(r_{ij} = 0, \tilde{p}_{ij}/p_0)} \quad (19)$$

where for the argument in U^{P} we took the most probable momentum $\tilde{p}_{ij} = \sqrt{m_e k_B T}$ of the pair of particles i, j . In the binary Slater sum for zero-particle distance $S_{ij}^0(r_{ij} = 0)$ we only took the Coulombic effects into account and left out the symmetry effects for identical particles since the symmetry effects are already included in the term $U^{\text{P}}(r_{ij} = 0, \tilde{p}_{ij}/p_0)$. Therefore we get

$$S_{ee}^0(r_{ee} = 0) = S_{pp}^0(r_{pp} = 0) = 4\sqrt{\pi} \xi_{ee} \int_0^{\infty} e^{-x^2} \frac{x dx}{1 - \exp \left\{ -\frac{\pi \xi_{ee}}{x} \right\}}. \quad (20)$$

The expression for $S_{ep}^0(r_{ep} = 0)$ is identical to $S_{ep}(r_{ep} = 0)$ which is given in Eq.(8) since there are no exchange effects between the two kinds of particles involved. In Fig. 1 we compare the shape of different potentials for the electron-electron interaction and for the electron-positron interaction. Here, all effective energies and the Coulomb energy are divided by the charge e_i in order to obtain the potential of the i -th particle with respect to the particle j . For simplicity, in the following the index i is skipped for all potentials. The original Kelbg potential V^{K} shows the right first derivative but does not have the correct height at $r_{ij} = 0$. The corrected KTR potential $V^{\text{KTR,corr}}$ has the

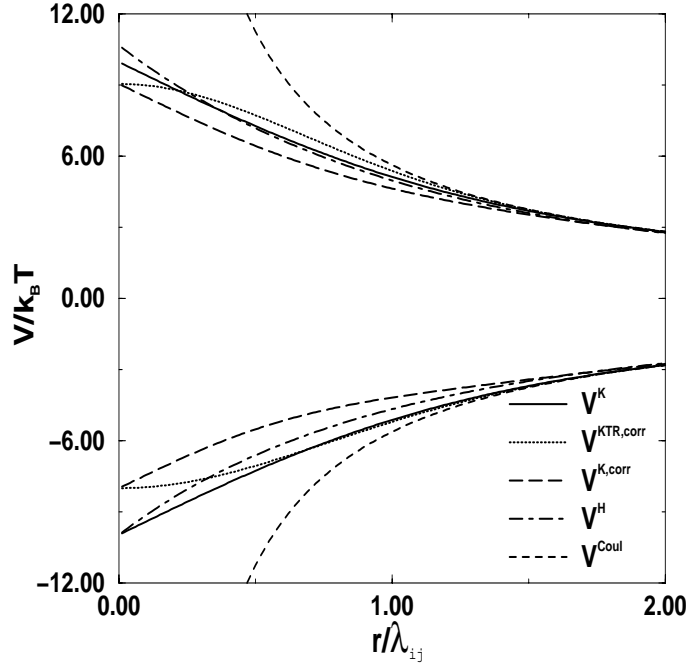


Fig. 1: Effective Potentials at $T = 10000 \text{ K}$; Kelbg potential V^K , corrected KTR potential $V^{KTR,corr}$ corrected Kelbg potential $V^{K,corr}$, Hansen potential V^H , and Coulomb potential V^{Coul}

correct height but not the right shape as $r_{ij} \rightarrow 0$. Also shown is the corrected Kelbg potential $V^{K,corr}$ Eqs.(3,5,10) which we use in our TCP simulations, the potential of Hansen *et al.* V^H ([14], see also work of C. Deutsch *et al.* [15]) and the Coulomb potential $V^{Coul} = e/4\pi\epsilon_0 r$.

Note that all effective potentials show the same long-range behaviour but differ for interesting short-range distances where correlations appear.

3 Monte Carlo simulations for the electron gas

Monte Carlo simulations were used to calculate the excess internal energy U^{xc} of a system consisting of N electrons as a function of Γ in the quasi-classical region (Fig. 2). Γ denotes the coupling parameter and is given by $\Gamma = e^2(4\pi n_e/3)^{1/3}/(4\pi\epsilon_0 k_B T)$, n_e is the electron density. The selected range of the coupling parameter Γ covers the region of weak coupling ($\Gamma \leq 10^{-2}$) up to the strongly coupled regime ($\Gamma = 30$).

For the classical OCP there exist analytical results for $U_{xc}(\Gamma)$ for $\Gamma \leq 0.4$ [16] and very accurate MC calculations in the region of strong coupling $1 \leq \Gamma \leq 200$ [4]. We compare our results to a Padé formula given by Kahlbaum [17] which covers the whole OCP fluid range $0 \leq \Gamma \leq 200$. Note that this Padé formula is limited to the pure classical plasma whereas our calculations include quantum effects through the effective potentials.

In Figs. 3 and 4 the pair-distribution function for a temperature of 20000 K and for different values of Γ is shown. While for $\Gamma = 0.5$ the distribution function increases monotonously to 1, for the strong coupled region ($\Gamma = 10$) it displays already a next-neighbour peak. The distances in the figures are given relatively the Bohr radius a_0 .

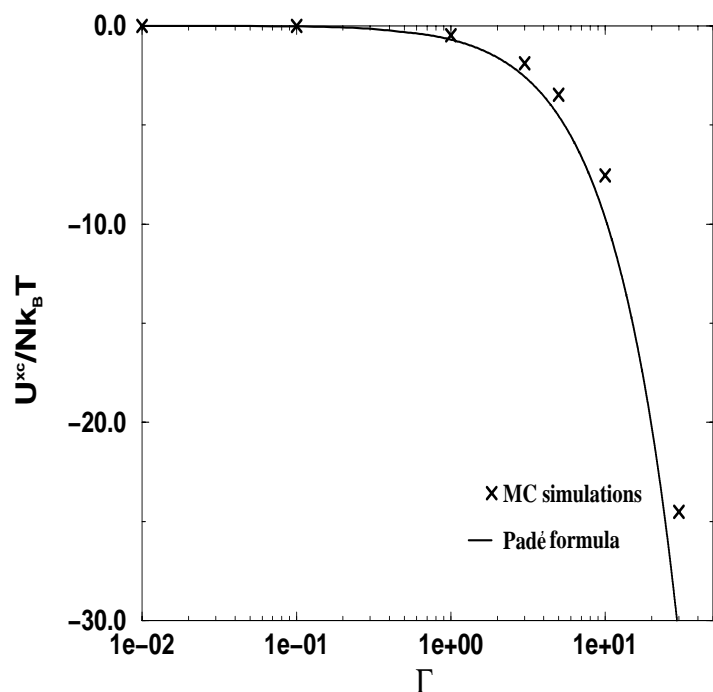


Fig. 2: Excess Internal Energy of the OCP

θ is the degeneracy and is given by $\theta = T/T_F$ where T_F is the Fermi temperature.

4 Monte Carlo simulations for mass-symmetrical plasmas

The equilibrium state of an electron-positron plasma is simulated using the corrected Kelbg potential $V^{K,corr}$ by a Monte Carlo run with 1600 particles. As a thermodynamic characteristic of TCP we present in Fig. 5 the effective energy

$$U^{eff} = \sum_{i<j} \frac{e_i e_j}{4\pi\epsilon_0} F(r_{ij}, m_{ij}, T, \gamma_{ij}) \quad (21)$$

and the Coulombic energy

$$U^{Coul} = \sum_{i<j} \frac{e_i e_j}{4\pi\epsilon_0 r_{ij}} \quad (22)$$

at a temperature of 10000 K as a function of Γ . The result for the corrected Kelbg potential of Eqs.(5,10) is compared with molecular dynamics simulations by Valuev [19, 20] ($U^{eff,V}$ and $U^{Coul,V}$), the classical Debye limit

$$U^{Debye} = -\sqrt{6}\Gamma^{3/2} Nk_B T \quad (23)$$

with N the number of electrons, and a Padé formula by Beule *et al.* [21] ($U^{Padé}$)

$$U^{Padé} = -Nk_B T \frac{\sqrt{6}\Gamma^{3/2}}{1 + \frac{1}{4}(6\pi)^{1/2}\Gamma^{3/2}\tau^{1/2}} \quad (24)$$

Here τ is given by

$$\tau = (2k_B T h^2 (4\pi\epsilon_0)^2 / m_{ep} e^4). \quad (25)$$

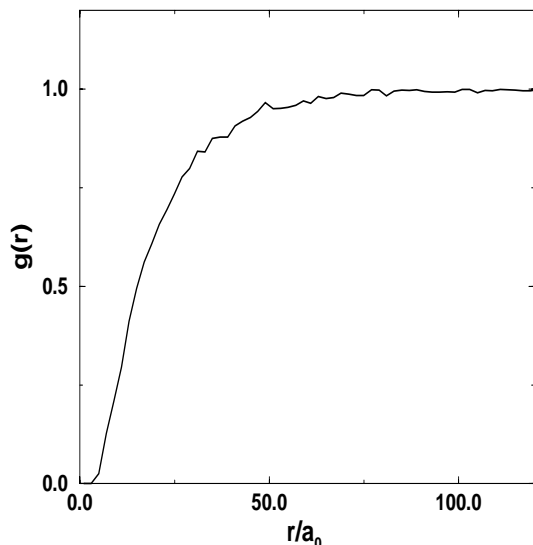


Fig. 3: $g_{ee}(r)$ for $T=20000$ K, $\Gamma=0.5$, $n_e = 5.1 \times 10^{19} \text{ cm}^{-3}$, $\theta = 34.3$

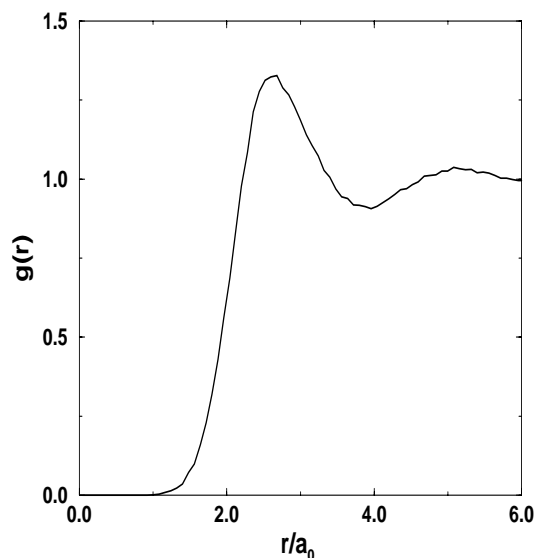


Fig. 4: $g_{ee}(r)$ for $T=20000$ K, $\Gamma=10$, $n_e = 4.1 \times 10^{23} \text{ cm}^{-3}$, $\theta = 0.08$

Pair-correlation functions for the electron-electron g_{ee} and the electron-positron g_{ep} correlations are shown in Figs. 6, 7 and 8 for three given temperatures: $T = 45500\text{K}$, $T = 98000\text{K}$, $T = 455000\text{K}$. For equal particles the electron-electron and positron-positron correlations are averaged over different spin directions. Since the masses of electrons and positrons are equal it yields one single curve. The results are compared with path integral Monte Carlo (PIMC) results [18] ($g_{ee,\text{PIMC}}$, $g_{ep,\text{PIMC}}$) and with molecular dynamics (MD) simulations [19] ($g_{ee,\text{MD}}$, $g_{ep,\text{MD}}$). For the given temperature region a qualitative agreement of all three methods is observed. Only for a limited range small divergences between the different results can be found.

5 Conclusion

An OCP and a mass symmetrical TCP was investigated by quasi-classical Monte Carlo simulations. The interactions between particles were simulated by effective pair potentials calculated by the method of Slater sums. We found the thermodynamic functions from simulations in good agreement with other simulation methods and with theoretical results. We could show that the pair-correlation functions are in good agreement with PIMC and MD methods. In a forthcoming paper we will skip the condition of equal masses and investigate the electron-proton plasma for a regime of strong coupling and partial degeneration.

Acknowledgements

We would like to thank Burkhard Militzer from the University of Illinois at Urbana-Champaign and Ilya Valuev from Moscow Institute of Physics and Technology for their kindly providing the simulation data.

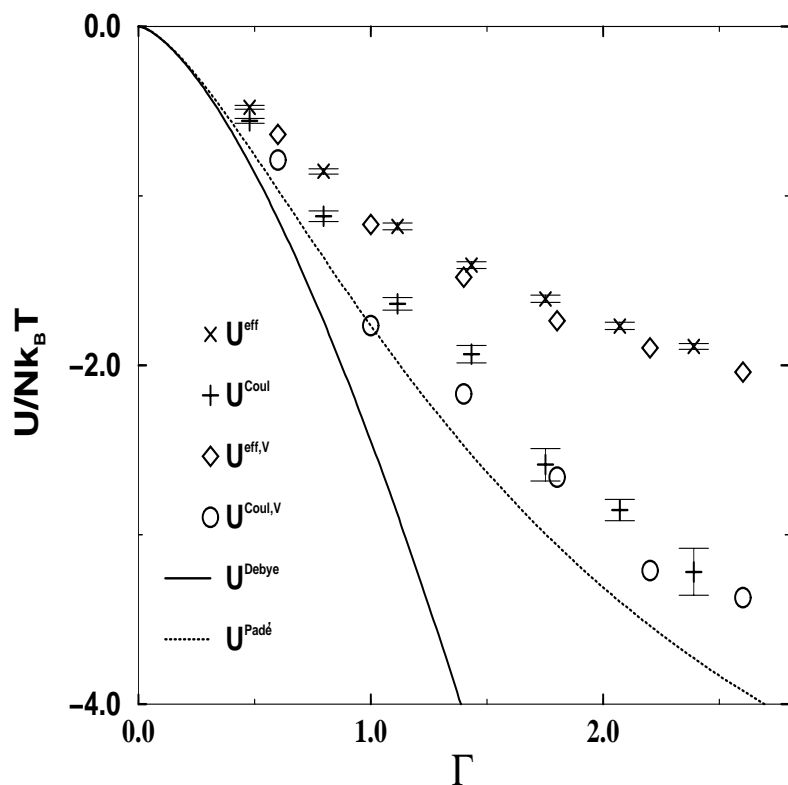


Fig. 5: Energies of TCP for various Γ at $T = 10000\text{ K}$; effective energy U^{eff} , Coulomb energy U^{Coul} , effective energy of simulations of Valuev $U^{eff,V}$, Coulomb energy of simulations of Valuev $U^{Coul,V}$, classical Debye results, and Padé' formula.

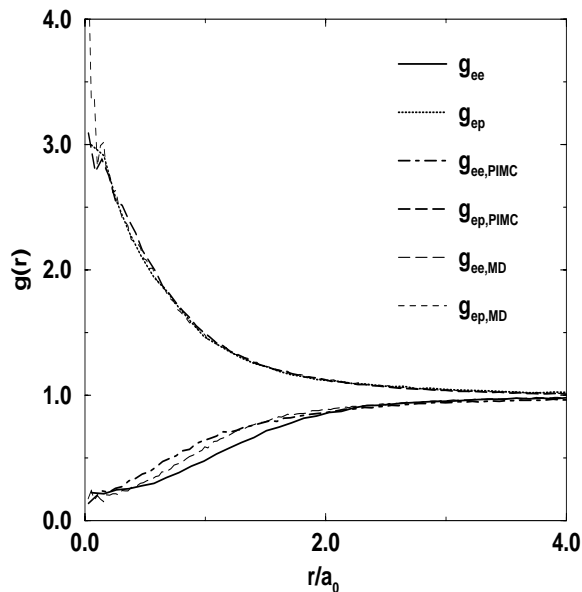


Fig. 6: Pair-distribution functions for the TCP at $T = 45500\text{ K}$, $n_e = 10^{23}\text{ cm}^{-3}$, $\Gamma = 2.7$, $\theta = 0.5$

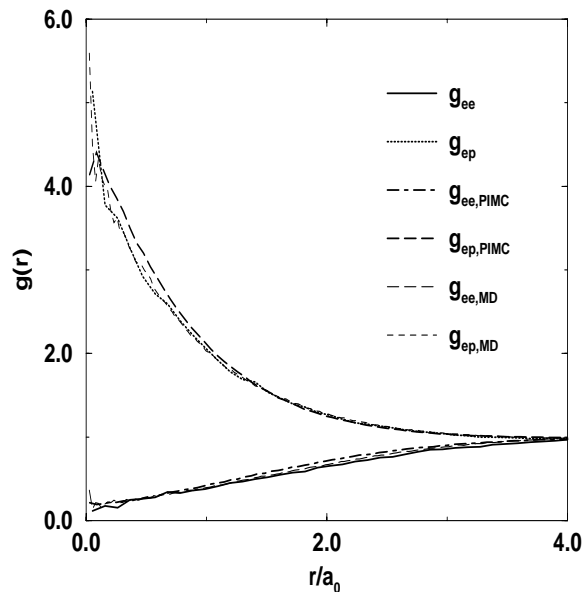


Fig. 7: Pair-distribution functions for the TCP at $T = 98000\text{ K}$, $n_e = 10^{22}\text{ cm}^{-3}$, $\Gamma = 0.59$, $\theta = 5$

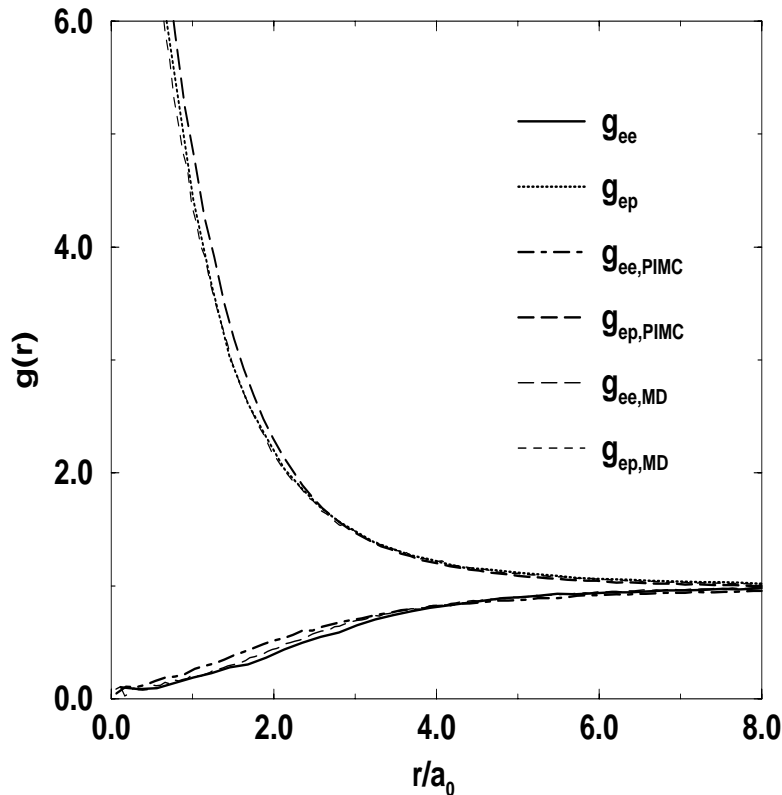


Fig. 8: Pair-distribution functions for the TCP at $T = 455000 \text{ K}$, $n_e = 10^{23} \text{ cm}^{-3}$, $\Gamma = 0.275$, $\theta = 5$

References

- [1] ICHIMARU, S., Rev. Mod. Phys. **54** (1982) 1017; ICHIMARU, S., HIROSHI, H., TANAKA, S., Phys. Rep. **149** (1987) 91
- [2] PERROT, F., DHARMA-WARDANA, M.W.C., Phys. Rev. **A 30** (1984) 2619
- [3] STOLZMANN, W., BLÖCKER, T., Astron. & Astrophys. **314** (1996) 1024
- [4] DEWITT, H.E., SLATTERY, W.L., STRINGFELLOW, G.S., in: *Strongly Coupled Plasma Physics*, ed. ICHIMARU, S., North-Holland, Amsterdam, 1990, p. 635
- [5] ZIMMERMANN, R., *Many-Particle Theory of Highly Excited Semiconductors*, TEUBNER-TEXTE zur Physik, Bd. 18, Teubner Verlagsgesellschaft, Leipzig, 1988
- [6] BLINNIKOV, S., DUNINA-BARKOVSKAYA, N.V., NADYOZHIN, D.K., Astrophys. J., Suppl. Ser. **106** (1996) 171
- [7] MORITA, T., Prog. Theor. Phys. **20** (1958) 920; **23** (1960) 829
- [8] KELBG, G., Ann. Phys. **12** (1963) 219
- [9] EBELING, W., KELBG, G., ROHDE, K., Ann. Phys. **21** (1968) 235
- [10] ROHDE, K., KELBG, G., EBELING, W., Ann. Phys. **22** (1968) 1; **25** (1970) 80
- [11] DORSO, C., DUARTE, S., RANDRUP, J., Phys. Lett. **B 188** (1987) 287
- [12] KLAKOW, D., TOEPFFER, C., REINHARD, P.-G., Phys. Lett. **A 192** (1994) 55
- [13] EBELING, W., SCHAUTZ, F., Phys. Rev. **E 56** (1996) 3498
- [14] HANSEN, J.P., McDONALD, I.R., Phys. Rev. **A 23** (1981) 2041, formula (16); Phys. Lett. **97 A** (1983) 42; BERNU, B., HANSEN, J.P., MAZIGHI, R., Phys. Lett. **100 A** (1983) 28
- [15] DEUTSCH, C., Phys. Lett. **60 A** (1977) 317; DEUTSCH, C., GOMBERT, M.M., MINOO, H., Phys. Lett. **66 A** (1978) 381; MINOO, H., GOMBERT, M.M., DEUTSCH, C., Phys. Rev. **A 23** (1981) 924

- [16] COHEN, E.G.D., MURPHY, T.J., *Phys. Fluids* **12** (1969) 1404
- [17] KAHLBAUM, T., in: *Physics of Strongly Coupled Plasmas*, ed. KRAEFT, W.D., SCHLANGES, M., World Scientific, Singapore, 1995, p. 99
- [18] EBELING, W., MILITZER, B., SCHAUTZ, F., *Contrib. Plasma Phys.* **30** (1997) 553
- [19] VALUEV, I.A., private communication (1999)
- [20] EBELING, W., NORMAN, G.E., VALUEV, A.A., VALUEV, I.A., *Contrib. Plasma Phys.* **39** (1999) 61
- [21] BEULE, D., EBELING, W., FÖRSTER, A., *Physica A* **241** (1997) 719